

5. K.W. Eccleston, Multiband power amplifier for multiband wireless applications, 3<sup>rd</sup> Int Conf Microwave Millimeter-wave Technol, Beijing, China, August, 2002, pp 1142–1145.
6. G.V. Eleftheriades, A.K. Iyer, and P.C. Kremer, Planar negative refractive index media using periodically L-C loaded transmission lines, IEEE Trans Microwave Theory Tech 50 (2002), 2702–2712.
7. H. Okabe, C. Caloz, and T. Itoh, A compact enhanced-bandwidth hybrid ring using a left-handed transmission-line section, IEEE MTT-S Int Microwave Symp Dig Philadelphia, PA (2003), 329–332.
8. Y. Ayasli, R.L. Mozzi, J.L. Vorhaus, L.D. Reynolds, and R.A. Pucel, A monolithic GaAs 1–13-GHz travelling-wave amplifier, IEEE Trans Microwave Theory Tech 30 (1982), 976–981.

© 2005 Wiley Periodicals, Inc.

## A NEW ELEMENT DESIGN FOR AN AXIS-INDEPENDENT, TUNABLE, NEGATIVE-PERMEABILITY ARTIFICIAL META-MATERIAL

Gong Ouyang and Vikram Jandhyala  
Applied Computational Electromagnetics Lab  
University of Washington  
Seattle, WA 98195

Received 27 August 2004

**ABSTRACT:** A new meta-material element that can realize axis-independent negative permeability is proposed and analyzed. The element is constructed as an intuitive 3D analog of the well-known flat split-ring structure (SRR). Unlike the SRR, the proposed element exhibits negative permeability for three preferred coordinate axes, and therefore enables meta-material applications such as focusing and efficient radiation from electrically small structures in multiple directions within the same structure. In addition, it is shown that the addition of lumped-circuit components to the element enables both tunability and functionality at very small sizes, far from the intrinsic resonance of the structure itself. The designed element is then simulated rigorously using a previously reported integral-equation technique that includes the ability to model linear and nonlinear tuning elements attached to the meta-material elements. © 2005 Wiley Periodicals, Inc. Microwave Opt Technol Lett 44: 530–533, 2005; Published online in Wiley InterScience (www.interscience.wiley.com). DOI 10.1002/mop.20687

**Key words:** meta-material; axis-independent; negative permeability; tenability; surface-integral equation

### INTRODUCTION

The design and analysis of negative-index materials, or meta-materials, has recently become a topic of great intellectual and practical interest. Several new and critical applications for focusing, radiation and antennas, transmission lines, and imaging are now being proposed. Negative-permeability materials are constructed by concentrating magnetic fields in a small region. In recent papers [1, 2], the split-ring structure (SRR) has been proposed and experimentally shown to exhibit negative permeability. One drawback of the SSR is that it is a planar structure, hence, its negative permeability behavior appears only when illumination is from a certain preferred direction. To attempt to remove or reduce this reduction, a more isotropic resonator structure, namely, the cross SRR (CSRR) has been proposed [3]. This structure exhibits negative permeability along two axes, by combining two orthogonally placed SRRs. In order to obtain a full three axes, and ultimately to obtain higher degrees of isotropy in negative-perme-

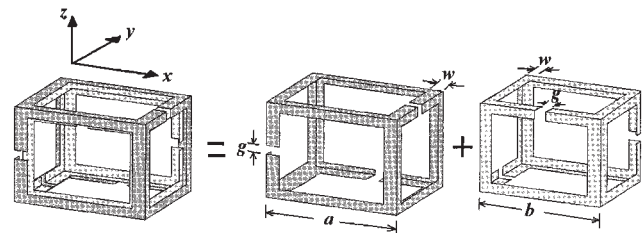


**Figure 1** Proposed 3D axis-independent meta-cube with three symmetric cuts in each of the two cubical frames and dimensions  $a = 4$  mm,  $b = 3.8$  mm,  $w = 0.4$  mm, and  $g = 0.4$  mm

ability behavior, SRRs of different sizes must be used due to geometrical constraints in creating the element without shorting metallic pieces. In such a configuration, each SRR must be retuned by adding separate tuning elements to match the frequency response of all the SRRs. Although possible, this is cumbersome. Moreover, if a three-axis independent element were available as a building block, rather than the single-axis SRR, this would enable immediate axis independence, and higher degrees of isotropy could be obtained by rotated versions of this three-axis structure. In this work, we propose such a 3D element that can, for the first time to the best of our knowledge, realize an axis-independent, frequency-matched, negative permeability material. Additionally, we show that once this element is used, it can be tuned to work at different frequencies away from the element's intrinsic resonance and can therefore enable electrically small applications, where such tuning will be most effective and useful. Finally, even higher degrees of isotropy can be obtained by combining rotated and scaled versions of the elements. The same caveats would then apply as in the CSRR case for higher isotropy, but this element would introduce three new negative permeability directions per instantiation, rather than just one.

The geometry of the proposed resonator, which is termed here the meta-cube, in keeping with its dual split cubical frame shape and its meta-material application, is shown in Figure 1. The structure is composed of two cubical frames, one inside the other. As Figure 1 shows, each cubical frame has three cuts in the middle of three edges. The two cubes are arranged in such a way that from each of the three preferred directions perpendicular to the cube faces, there appears a two-element stacked rectangular SRR. The stacked split-ring resonator (SSRR), a planar one-directional meta-material element has recently been analyzed in detail by other researchers [4]. For the stacked SRR in this cubic structure, it is easy to see that the two rings are placed perpendicular to each other, instead of using the conventional opposite placement. Since the size of each stacked SRR is the same, the scaling problem one would encounter in a higher-degree isotropy CSRR is circumvented. Furthermore, the structure is completely symmetric for specific finite rotations. For example, the structure repeats after rotation of  $\pi/2$  about the  $x$ -axis, followed by  $\pi/2$  about the  $y$ -axis. This kind of symmetry in geometry also lends itself to ensuring axis-independence of the associated meta-material. The specific dimensions proposed in this paper are as follows:  $a = 4$  mm,  $b = 3.8$  mm,  $w = 0.4$  mm, and  $g = 0.4$  mm. The spacing between the inner and outer cubical frames is only 0.1 mm, which implies strong field-coupling between the two frames.

### GENERALIZED CONSTITUTIVE RELATION AND COUPLED CIRCUIT-ELECTROMAGNETIC FORMULATION

The following simulation methodology, a rigorous extension to coupled circuit-electromagnetic simulation of a previous experi-

mentally validated electromagnetic-simulation technique that was developed collaboratively by the authors [5], is summarized here and will be detailed in a future paper. This methodology is based on surface integral equations, circuit-level lumped models, and generalized tensor constitutive relations, and enables both broadband and narrowband simulation of regular and tunable meta-material structures.

Strong cross-magnetolectric and electromagnetic effects are expected from the meta-cube elements, and therefore the starting point is the  $6 \times 6$  matrix-tensor constitutive relation for bianisotropic media:

$$\begin{bmatrix} \mathbf{D} \\ \mathbf{H} \end{bmatrix} = \begin{bmatrix} \boldsymbol{\varepsilon}_p & \boldsymbol{\alpha} \\ \boldsymbol{\beta} & \boldsymbol{\mu}_p^{-1} \end{bmatrix} \begin{bmatrix} \mathbf{E} \\ \mathbf{B} \end{bmatrix}, \quad (1)$$

where the tensors  $\boldsymbol{\varepsilon}_p$ ,  $\boldsymbol{\alpha}$ ,  $\boldsymbol{\beta}$ , and  $\boldsymbol{\mu}_p^{-1}$  are used to couple the electric field  $\mathbf{E}$  and magnetic induction  $\mathbf{B}$  with the electric displacement  $\mathbf{D}$  and magnetic field  $\mathbf{H}$ . For the purpose of building a 3D material with the 3D meta-cube element, a periodic 3D array of the meta-cube structure is simulated with an interelement centroid-centroid spacing along all coordinate axes of 5.5 mm. If the spacing between such elements is indeed less than one-tenth of the wavelength of an incident wave, a generalized constitutive-relation effective dipole approximation can be applied with excellent accuracy [5]. This relation is given by

$$\begin{bmatrix} \boldsymbol{\varepsilon}_p & \boldsymbol{\alpha} \\ \boldsymbol{\beta} & \boldsymbol{\mu}_p^{-1} \end{bmatrix} = \begin{bmatrix} \varepsilon_0 \boldsymbol{\varepsilon}_b \mathbf{U} & \mathbf{O} \\ \mathbf{O} & \frac{1}{\mu_0} \mathbf{U} \end{bmatrix} + N \begin{bmatrix} \mathbf{U} & \mathbf{O} \\ \mathbf{O} & -\mathbf{U} \end{bmatrix} \bar{\boldsymbol{\alpha}} \left( \begin{bmatrix} \mathbf{U} & \mathbf{O} \\ \mathbf{O} & \mathbf{U} \end{bmatrix} - N \begin{bmatrix} \frac{1}{\varepsilon_0 \boldsymbol{\varepsilon}_b} \mathbf{C} & \mathbf{O} \\ \mathbf{O} & \mu_0 \mathbf{C} \end{bmatrix} \bar{\boldsymbol{\alpha}} \right)^{-1}, \quad (2)$$

where  $\bar{\boldsymbol{\alpha}}$  is a  $6 \times 6$  polarizability matrix which is obtained directly from the electric- and magnetic-dipole moments of a single meta-cube element,  $\mathbf{C}$  is the interaction matrix of the array which is related to the spacing between elements,  $\mathbf{U}$  is a  $3 \times 3$  identity matrix, and  $N$  is the volumetric concentration of the material. The magnetic- and electric-dipole moments for the meta-cube are obtained by

$$\mathbf{p}_e = \frac{1}{j\omega} \int \mathbf{J}(\mathbf{r}, \omega) ds, \quad (3a)$$

$$\mathbf{p}_m = \frac{1}{2} \int \mathbf{r} \times \mathbf{J}(\mathbf{r}, \omega) ds, \quad (3b)$$

where  $\mathbf{J}(\mathbf{r}, \omega)$  is the equivalent-surface current density in the frequency domain.

To calculate the induced surface current under EM illumination, a coupled EM-circuit formulation is used to calculate the induced surface current on the cube [6]. The cubic structure is simulated as an EM object while the lumped-circuit element connected to it is simulated by a SPICE-like circuit-level solver. The coupling between the EM and circuit modeling is through a rigorously defined 3D terminal that is used to enforce potential matching, and Kirchoff's Current Law (KCL) is also applied to guarantee the charge conservation. The coupled system in final matrix form is

$$\begin{bmatrix} \mathbf{Z}_0^{\text{II}} & \mathbf{Q}_0^{\text{II}} & \bar{\mathbf{0}} \\ \mathbf{Z}_0^{\text{II}} & \mathbf{Q}_0^{\text{II}} & \bar{\mathbf{C}} \\ \bar{\mathbf{0}} & \bar{\mathbf{C}}^{\text{T}} & \text{MNA}_0 \end{bmatrix} \begin{bmatrix} \mathbf{J}(t_j) \\ \mathbf{I}(t_j) \\ \text{ckt}(t_j) \end{bmatrix} = \sum_{i=1}^j \begin{bmatrix} \mathbf{Z}_i^{\text{II}} & \mathbf{Q}_i^{\text{II}} & \bar{\mathbf{0}} \\ \mathbf{Z}_i^{\text{II}} & \mathbf{Q}_i^{\text{II}} & \bar{\mathbf{0}} \\ \bar{\mathbf{0}} & \bar{\mathbf{0}} & \text{MNA}_i \end{bmatrix} \times \begin{bmatrix} \mathbf{J}(t_{j-i}) \\ \mathbf{I}(t_{j-i}) \\ \text{ckt}(t_{j-i}) \end{bmatrix} + \begin{bmatrix} \text{src}_{EM}(t_j) \\ \mathbf{0} \\ \text{src}_{CK}(t_j) \end{bmatrix}, \quad (4)$$

where  $\mathbf{J}(t_j)$ ,  $\mathbf{I}(t_j)$ , and  $\text{ckt}(t_j)$  are the EM current unknowns, branch current unknowns and circuit unknowns at time  $t_j$ , respectively, and  $\text{src}_{EM}(t_j)$  and  $\text{src}_{CK}(t_j)$  are the EM and circuit excitations, respectively. In matrices appearing in the above equation,  $\mathbf{Z}^{\text{II}}$  and  $\mathbf{Q}^{\text{II}}$ , respectively, describe the contribution to the electric field from the EM currents and branch currents injected into the EM object from the circuit nodes,  $\mathbf{Z}^{\text{II}}$ ,  $\mathbf{Q}^{\text{II}}$ , and  $\mathbf{C}$  are used to enforce the potential matching condition on terminal basis functions,  $\text{MNA}$  is used to describe the modified nodal analysis of the circuit simulation part, and the sparse matrix  $\mathbf{C}^{\text{T}}$  is used to enforce KCL between currents.

## NUMERICAL RESULTS

In the presented simulation results, a transient Gaussian-shaped plane wave is used as the excitation. The surface-current unknowns are obtained at each time step by solving Eq. (4). After a Fourier transform, Eqs. 3(a), 3(b), and finally (2) are used to obtain the permeability in the axial  $x$ ,  $y$ , and  $z$  directions.

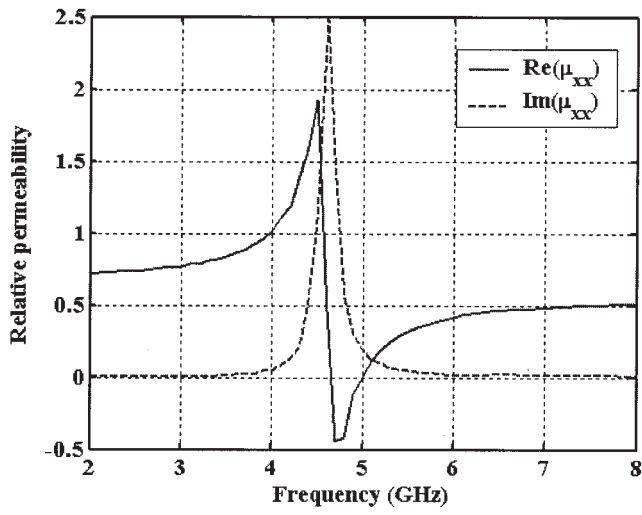
First, the meta-cube is simulated without any tuning circuit elements. The permeability is described by a  $3 \times 3$  tensor and, for each permeability component, it is defined in the form  $\mu = \mu' - j\mu''$ . Figures 2(a)–2(c) show both the real and imaginary parts of permeability versus frequency. A negative real part of permeability is observed in these curves near the resonant frequency of about 4.7 GHz. Importantly, the three figures are nearly identical, thus demonstrating the axis-independent property of the meta-cube.

The size of the meta-cube is then reduced to one-tenth the original size, and the spacing between elements is reduced by the same factor. A 2-pF capacitor is inserted at each gap. As Figures 3(a)–3(c) show, after the scaling and insertion of the capacitors, the negative-real permeability and axis independence are preserved. Also, the resonance region is around 3.1 GHz, which is less than a 30% reduction in frequency, even though the structure has been scaled down by a factor of 10.

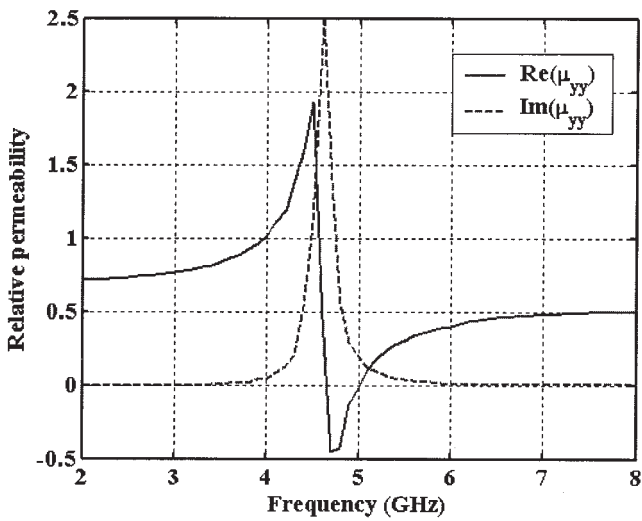
To demonstrate the tunability of the circuit-coupled meta-cube, the value of capacitor is changed to 1 pF. Figure 4 shows the resonance shift, from 3.1 to 4.5 GHz, due to the different capacitance. In other words, the modified capacitance has retuned the meta-cube to almost the same resonance as the unscaled version. A further potential application includes using different tuning elements in different gaps in order to obtain varying behaviors along each axis.

## CONCLUSION

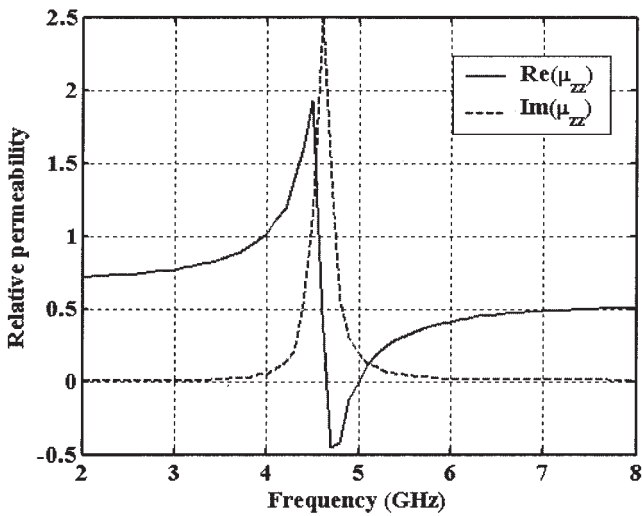
To conclude, a highly axis-independent magnetic resonator, the meta-cube, has been proposed to realize negative permeability in the three axial directions. Through a rigorous numerical simulation, axis independence, negative permeability, and tunability have been demonstrated. The meta-cube has the potential ability to result in materials that have strong multidirectional meta-material properties, and applications in substrates for electrically-small radiating structures.



(a)

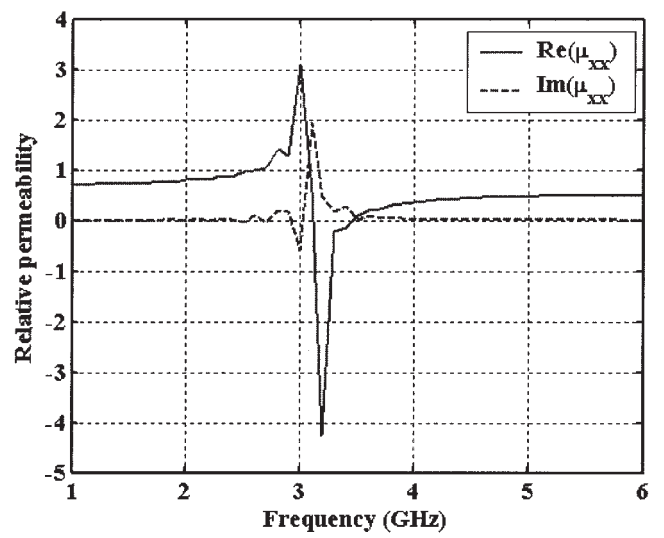


(b)

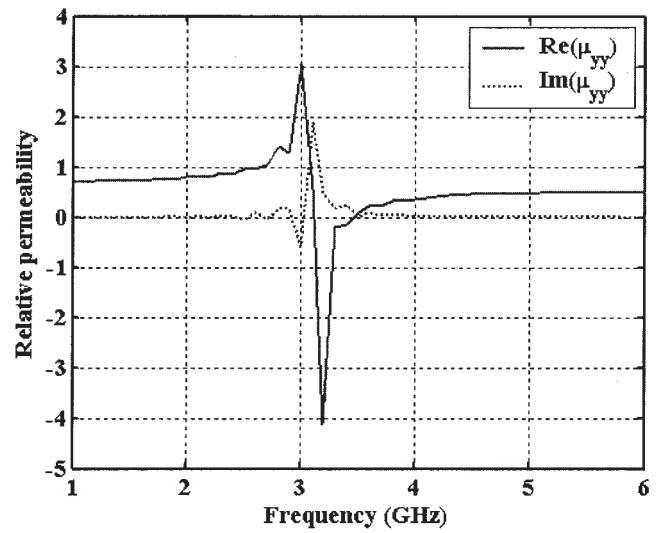


(c)

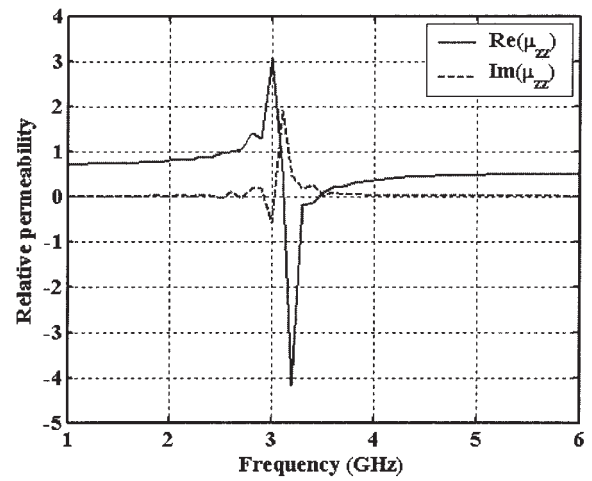
**Figure 2** Negative permeability of the meta-cube showing permeability in the (a) x, (b) y, and (c) z directions



(a)



(b)



(c)

**Figure 3** Negative permeability of 1/10 scaled meta-cube with 2-pF capacitors showing permeability in the (a) x, (b) y, and (c) z directions

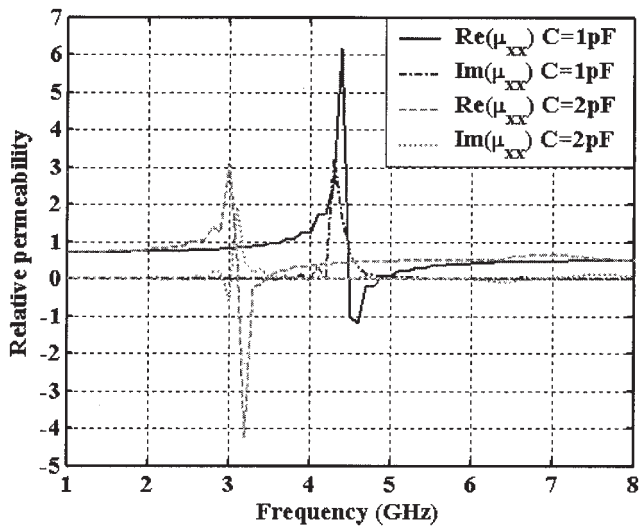


Figure 4 Demonstration of the tunability of the meta-cube

#### REFERENCES

1. J.B. Pendry, A.J. Holden, D.J. Robbins, and W.J. Stewart, Magnetism from conductors and enhanced nonlinear phenomena, *IEEE Trans Microwave Theory Tech* 47 (1999), 2075–2084
2. D.R. Smith, W.J. Padilla, D.C. Vier, S.C. Nemat-Nasser, and S. Schultz, A composite medium with simultaneously negative permeability and permittivity, *Phys Rev Lett* 84 (2000), 4184–4187.
3. P. Gay-Balmaz and O.J.F. Martin, Efficient isotropic magnetic resonators, *Appl Phys Lett* 81 (2002), 639–641.
4. S.W. Lee, A. Ishimaru, Y. Kuga, and V. Jandhyala, Combined numerical and analytic approach for generalized models of complex bi-anisotropic materials, *Proc SPIE* 4806 (2002), 92–99.
5. A. Ishimaru, S.W. Lee, Y. Kuga, and V. Jandhyala, Generalized constitutive relations for metamaterials based on the quasi-static Lorentz theory, *IEEE Trans Antennas Propagat* 51 (2003), 2550–2557.
6. C. Yang and V. Jandhyala, Coupled circuit-electromagnetic simulation with time domain integral equations, *Antennas Propagat Soc Int Symp* 3 (2003), 316–319.

© 2005 Wiley Periodicals, Inc.

## A NEW PLANAR-TYPE DIELECTRIC RESONATOR USING LTCC TECHNOLOGY FOR mm-WAVE BAND APPLICATIONS

Sanghee Kim,<sup>1,2</sup> Jounghyun Yim,<sup>1</sup> and Bumman Kim<sup>1</sup>

<sup>1</sup> Department of Electrical Engineering and Microwave Application Research Center

Pohang University of Science and Technology  
San 31, Hyoja Dong, Nam Gu  
Pohang, 790-784, Republic of Korea

<sup>2</sup> Intechwave Inc.

501 Ace Techno-Tower 1  
197-17, Guro Dong, Guro Gu  
Seoul, 152-848, Republic of Korea

Received 26 August 2004

**ABSTRACT:** A new planar-type dielectric resonator (PDR) with a high unloaded  $Q$  has been developed using LTCC Technology. The PDR consists of two different dielectric constant materials, high dielectric LTCC cavity ( $\epsilon_r = 36$ ) acting as a resonator and low dielectric LTCC layer ( $\epsilon_r = 5.2$ ) surrounding the cavity. Also, the layer has staggered air holes on the top

and bottom of the resonator instead of the air cavity of the original PDR, a hollow patch center ground plane at the middle, and shielded cavity metals. The newly realized PDR structure shows a high unloaded  $Q$  of about 6212 at 37.3 GHz and the measured results are in good agreement with the simulated ones. The PDR can be easily integrated into a planar circuit and can be applicable to mm-wave band systems. © 2005 Wiley Periodicals, Inc. *Microwave Opt Technol Lett* 44: 533–536, 2005; Published online in Wiley InterScience (www.interscience.wiley.com). DOI 10.1002/mop.20688

**Key words:** DR; PDR; staggered air hole; LTCC

#### 1. INTRODUCTION

A high unloaded  $Q$  ( $Q_u$ ) resonator is essential for low-phase noise oscillators and high  $Q$  filters [1]. In mm-wave-band, dielectric resonators (DR) are widely used to get a high unloaded  $Q$ . The requirements of the DR are high unloaded  $Q$ , small size, low insertion loss, high temperature stability, productivity, and low cost. Recently, a planar-type dielectric resonator (PDR) using a high dielectric substrate, which can deliver a high unloaded  $Q$  and be easily integrated with multilayer MICs, has been reported [2–4]. For a PDR operating in the  $TE_{010}$  mode, most of the electromagnetic field energy is confined inside the DR and decreased exponentially outside the DR. Those PDRs have been reported to have a high unloaded  $Q$  of about 1610. However, the unloaded  $Q$  is rather low compared to the dielectric resonator because a strong electromagnetic field is formed at the edge of the ground plane, where a significant metal loss is generated and the unloaded  $Q$  of the PDR is degraded. Among substrate technologies, low-temperature co-fired ceramic (LTCC) technology is attracting microwave and mm-wave engineers' attention due to the 3D integration capability for size reduction and low cost, and the small-dielectric-loss tangent [5, 6].

This paper proposes a new PDR based on LTCC technology with a high-dielectric resonator embedded in a low-dielectric material in order to meet most of the above requirements. Our LTCC PDR has a disk-shaped high-dielectric LTCC cavity and one hollow-patch ground plane located at the center of a low-dielectric LTCC layer with staggered air holes at the top and bottom of the resonator. The PDR has a significantly improved unloaded  $Q$  and reduced size, as compared to other PDRs. Also, it has a merit of manufacturability because it does not need any separate air gap or

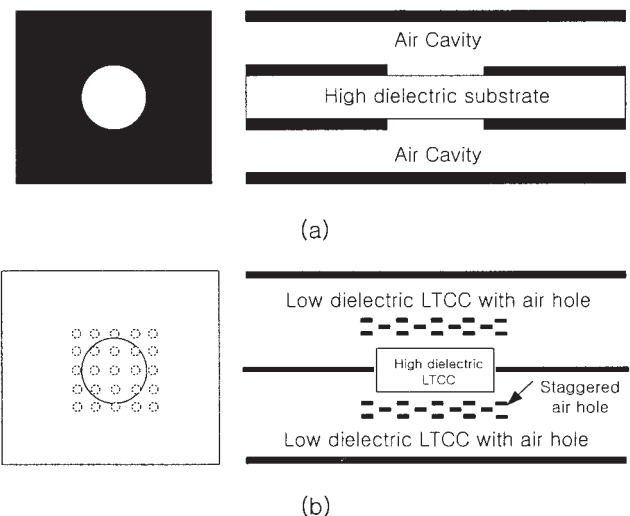


Figure 1 Configurations of PDRs (a) PDR with double ground (b) proposed LTCC PDR with staggered air hole.